Magnetic properties and critical behavior of quasi-two-dimensional systems $[C_6H_5(CH_2)_nNH_3]_2CuBr_4$ with $n=1$, 2, and 3

P. Zhou and John E. Drumheller
Department of Physics, Montana State University, Bozeman, Montana 59717

Baldev Patyal* and R. D. Willett
Department of Chemistry, Washington State University, Pullman, Washington 99164
(Received 3 June 1991)

The magnetic properties and critical behavior of the quasi-two-dimensional ferromagnets $[C_6H_5(CH_2)_nNH_3]_2CuBr_4$, with $n=1$, 2, and 3, have been studied. These compounds are typical of layered magnets in that they assume distorted layer perovskite structures in which copper(II) bromide layers are sheathed by the bulk organic cations. Magnetization and susceptibility measurements show strong ferromagnetic intralayer exchange of the order of 20–25 K with weak interlayer exchange coupling of less than 1 K. The magnetic anisotropies are explored through EPR-linewidth analysis. The critical exponent γ and transition temperatures T_c were determined by the measurements of ac initial susceptibility and isothermal magnetization. By employing a static scaling law to analyze the data of isothermal magnetizations near T_c, it was found that in a certain low-field and low-temperature region the powder magnetizations are suppressed so that the scaling hypothesis no longer holds. It is shown from the scaling analysis that the powder samples of these two-dimensional (2D) layer ferromagnets cannot be classified as simple ferromagnets whose critical behavior is described by the usual 2D critical theories.

I. INTRODUCTION

The magnetic properties and critical behavior in layer perovskite-type transition-metal salts with the general formula $(RNH_3)_2MX_4$ (R =an organic functional group, M =a divalent metal ion, and X = a halide F^-, Cl^-, or Br^-) have been of particular interest for more than two decades.[1–10] Since a rich variety of nonmagnetic organic cations produce large and variable separation between the magnetic metallate layers, many attempts have been made using these compounds to verify theoretical predictions about two-dimensional (2D) and quasi-2D magnetic systems. It is now firmly established that the phase transition for the ideal 2D Heisenberg system at nonzero temperature is not related to long-range order, even though it is characterized by an infinite initial susceptibility.[11–14] In contrast, quasi-2D ferromagnets, which are systems that deviate from ideal isotropic 2D systems by the introduction of spatial anisotropies and spin anisotropies, are well known to have a finite transition temperature related to the onset of long-range order.[15–20] Thus, the behavior of spontaneous magnetization and the degree of divergence of the initial susceptibility at the transition temperature play an important role in indicating the difference of the critical behavior between the real quasi-2D system and the ideal isotropic 2D system. Recently, on the theoretical side, 2D critical theories have been extensively developed[21–32] and, in particular, the principle of conformal invariance has led to remarkable progress in the theory of 2D critical phenomena.[33–38] The classification of 2D critical theories may be universally characterized by what is called the conformal anomaly.[35,36] Such applications of conformal invariance in 2D critical theories require that a system of short-range interactions at the critical point is not only scale invariant but also translationally and rotationally invariant.[34,36] Although no experimental work has been reported to verify the 2D conformal critical theory so far, it is possible to verify the applicability of such "universal" 2D critical theory for a realistic 2D system by testing the scaling invariance from the critical-point data.

The magnetic susceptibilities of the series of $(RNH_3)_2CuX_4$ compounds with $X=Cl^-$ or Br^- are characterized by nearly Heisenberg ferromagnetic intralayer coupling, with a small 1–5% XY (Cl) or Ising (Br) anisotropy. The interlayer coupling is generally very weak, especially for large R groups, and both ferromagnetic and antiferromagnetic interlayer coupling are observed. The class of compounds $[C_6H_5CH_2)_nNH_3]_2CuCl_4$ have been reported to belong to the rare group of insulating three-dimensional (3D) ferromagnets.[39,40] A detailed electron paramagnetic resonance (EPR) study of these compounds was recently undertaken to probe their local anisotropies. One feature of this study was the observation of effects due to magnetically inequivalent layers which implied that the interlayer coupling was less than 10^{-3} K.[41]

In this work, we report the studies of the magnetizations and susceptibilities of these quasi-2D ferromagnets $[C_6H_5(CH_2)_nNH_3]_2CuBr_4$ with $n=1$, 2, and 3. In addition we attempt to analyze isotherm data near the T_c by employing the static magnetic equation of state. EPR studies are reported, and the EPR linewidths are analyzed in terms of the contributions of the anisotropic and antisymmetric components of the exchange coupling.

II. EXPERIMENTAL PROCEDURE

A. Preparation of samples

The samples of $[C_6H_5(CH_2)_nNH_3]_2CuBr_4$ were prepared and crystals grown in the following manner. For the $n=1$ salt, 0.03 mol (5.6 g) of the benzylammonium bromide powder and 0.015 mol (3.4 g) of $CuBr_2$ (stoichiometric amounts) were dissolved in methanol. The best crystals were grown in a constant air flow apparatus. The opaque crystals are hygroscopic and must be dried under vacuum and stored in an air-tight dry container. To prepare the $n=2$ salt, 0.03 mol (6.1 g) of phenethylammonium bromide and 0.15 mol (3.4 g) of $CuBr_2$ were dissolved in 20% aqueous HBr. After about 20 days of slow evaporation, very poor quality crystals were formed. These crystals were then redissolved in ethanol and left for slow evaporation again. Good crystals were grown in about a month. These crystals are in the form of dark, shiny nonhygroscopic plates. For $n=3$, a similar procedure starting with 0.0146 mol (3.16 g) of 3-phenyl-1-propylammonium bromide and 0.073 mol of $CuBr_2$ yielded good quality nonhygroscopic crystals.

B. Crystal structure description

Small single crystals of each salt were mounted on a Nicolet R3m diffractometer for x-ray analysis. Extreme care had to be taken in handling the crystals because of their extremely fragile nature. Lattice constants and probable space groups were determined (Table I). A structure determination has been completed for the $n=2$ system,[42] complete structure determinations for the other two compounds are in progress.

All three salts contain antiferrodistortive layers of planar $CuBr_4^{2-}$ anions separated by the double layers of the $C_6H_5(CH_2)_nNH_3^+$ cations. This arrangement leads to a tetragonally elongated octahedral arrangement for each Cu^{2+} ion. The structure of the $n=2$ compound[42] is isostructural with that of $(C_2H_5NH_3)_2CuCl_4$.[43] The layer arrangement is shown in Fig. 1. From the space-group symmetry, adjacent layers are related by a glide-plane operation, and thus are magnetically inequivalent. The structures of the $n=1$ and $n=3$ salts are not known in detail, but several features need to be noted. The in-plane crystallographic axes for $n=1$ are rotated by 45° with respect to those for the $n=2$ structure, doubling the size of the repeat unit within the layer. The length of the c axis is also doubled, leading to a four layer repeat in that direction, so that adjacent layers will not be structurally or magnetically equivalent. The space group $P\bar{1}$ for the $n=3$ salt implies the presence of two sets of structurally

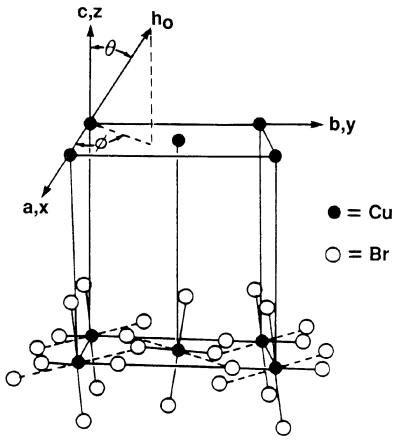

FIG. 1. Illustration of the layer structure in $(CH_6H_5C_2H_4NH_3)_2CuBr_4$. The a axis is out of the plane of the illustration.

or magnetically inequivalent layers. In all cases, the large interlayer separation insures the presence of only dipolar coupling between layers.

C. Magnetic measurements

All measurements of magnetizations and dc susceptibilities reported in this work were performed on the EG&G Model 155 Vibrating Sample Magnetometer (VSM) with a variable-temperature helium cryostat system. The magnetometer was calibrated with a nickel crystal obtained from the National Bureau of Standards. The zero-field ac susceptibility was carried out by an ac mutual inductance bridge using a superconducting quantum interference device (SQUID) as a flux detector. A bridge frequency of 80 Hz was used. The accuracy of zero-field was estimated to be about ±1.0 Oe.

Powder samples of 101, 96, and 91 mg for $n=1$, 2, and 3, respectively, were measured. The isothermal magnetization measurements were performed in the field range $0<H<4000$ Oe from 2.9 to 35 K. A full linear dependence of the magnetization vs field up to 5000 Oe was found above approximately 19 K for all compounds. Thus, the susceptibility vs. temperature above 20 K was obtained from the direct measurement of the magnetization at an applied field 5000 Oe.

All EPR measurements of crystals were made with a Varian E-3 EPR spectrometer. Measurements were made at both room temperature and liquid-nitrogen temperature (77 K). Crystallographic axes were identified using a precession camera. Data was collected about three

TABLE I. Lattice constants and probable space groups for $[C_6H_5(CH_2)_nNH_3]_2CuBr_4$ salts.

	a (Å)	b (Å)	c (Å)	α (°)	β (°)	γ (°)	Probable space group
$n=1$	10.558	10.486	63.473	90	98.08	90	$A2/a$
$n=2$	7.654	7.756	38.042	90	90	90	$Pcab$
$n=3$	7.774	7.804	39.350	90.89	100.77	88.54	$P\bar{1}$

mutually perpendicular axes by remounting the crystals appropriately on the goniometer.

III. RESULTS AND DISCUSSIONS

A. Powder magnetizations and susceptibilities

The isothermal magnetization data of powdered samples at several different temperatures were obtained with the field swept from 3000 to 0 Oe and are shown as points in Fig. 2 for $n=1$. A similar behavior was seen for $n=2$ and $n=3$. Hysteresis at low temperatures indicate ferromagnetic behavior with approach to saturation beyond about 3000 Oe. As temperature increases, the remnant magnetizations and coercive forces decrease. The remnant magnetizations are relatively small, which implies that the magnetizations, shown at low field in Fig. 2 for $n=1$, are suppressed compared with those for usual 3D amorphous ferromagnets. This feature will be clear in Sec. III *C* below when we apply the static scaling law to analyze the isothermal magnetization data.

The magnetization vs temperature in several different applied fields are shown in Fig. 3 for $n=1$, with similar behavior observed for $n=2$ and $n=3$. All of the samples were measured from 4.2 to about 35 K in fields up to 5000 Oe. At low temperatures, the gradually increasing values of magnetization as the temperature decreases show that these compounds order mainly ferromagnetically. The magnetization of the $n=2$ sample is weaker than that of the $n=3$ sample at relatively high fields and at low temperatures.

The susceptibility in the temperature range from 20 to 200 K was obtained from the measurements of magnetization vs temperature at an applied field 5000 Oe and are shown as solid points in Fig. 4 for $n=1$. The data were fitted to a high-temperature series expansion for the eclipsed 3D Heisenberg model that included both J (nearest intralayer exchange) and J' (nearest interlayer exchange). A nonlinear optimization program was used to minimize the standard deviation between the experimental and the calculated susceptibility with J and J' as

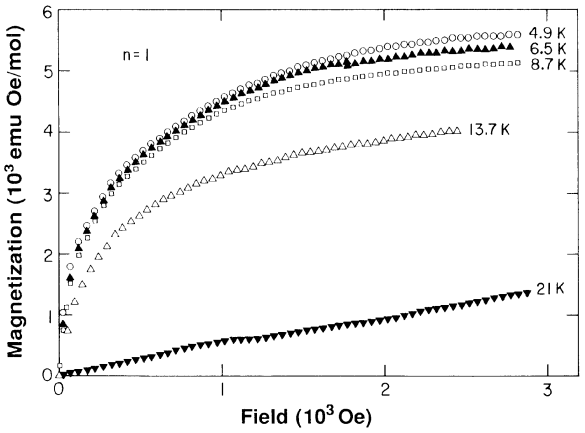

FIG. 2. Isothermal magnetization vs field at several different temperatures for the powdered samples of $[C_6H_5(CH_2)_nNH_2]_2CuBr_4$ with $n=1$.

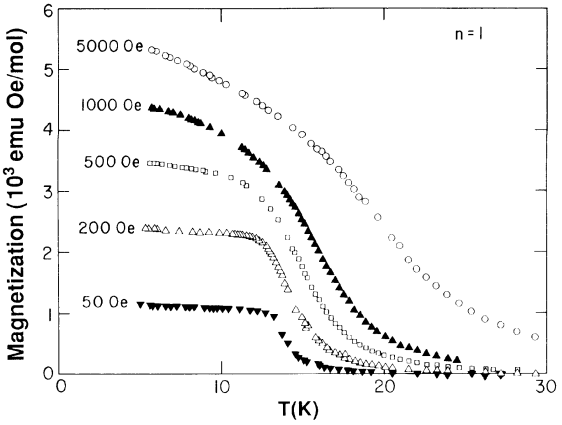

FIG. 3. Magnetizations vs temperature at several different applied fields for the $n=1$ powdered sample.

variables. In order to make the truncation of high-temperature expansion valid up to fourth order, we have chosen the minimum temperature to which the data were fitted to be a value of $J/k_BT=0.70$. The calculated results corresponding to the best fit for $n=1$ are shown as the solid line in Fig. 4. The values of J are summarized in Table II for $n=1$, 2, and 3. It should be pointed out that the two-parameter fit was insensitive to the small interlayer exchange coupling J', which means that the values of J' obtained here are not sufficiently reliable. Possible upper-bound values of $|J'|$ are listed in Table II.

The zero-field ac susceptibility vs temperature data are shown as the points in Fig. 5. It is clear from Fig. 5 that there is a peak corresponding to the transition temperature T_c indicative of a second-order phase transition. For a simple ferromagnet, the zero-field susceptibility at the demagnetized state ($M=0$ $H=0$), the so-called initial susceptibility, is usually expected to be divergent at $T=T_c$. However, due to the spin and lattice anisotropies and the

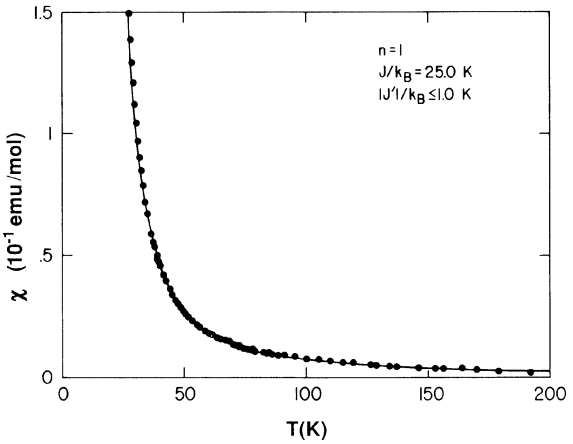

FIG. 4. Magnetic susceptibility vs temperature for the $n=1$ powdered sample. The solid line is the best-fit result calculated by a high-temperature series of expansion with $J/k_B=25.0$ K and $|J'|/k_B<1.0$ K.

TABLE II. Summary of magnetic anisotropies and T_c in 2D layer perovskite systems.

Compound	T_c (K)	J/k_B (K)	$\lvert J'\rvert/k_B$ (K)	$\lvert d_x/d_y\rvert$	$\left\lvert\frac{(d_z^2+RD^2)^{1/2}}{d_y}\right\rvert$
$n=1$	12.81	25.0	<1.0	1.00	1.24
$n=2$	12.85	22.7	<0.5	1.31	1.45
$n=3$	10.02	21.1	<0.3		

demagnetization effect, many ferromagnets do not show this divergence. It is clear from Fig. 5 that there is no sharp divergence for these powdered samples particularly for the $n=3$ compound. So far there are no exact general expressions for the susceptibilities of the quasi-2D systems. For most of the ferromagnetic copper layer compounds with a weak antiferromagnetic interlayer exchange, the 3D ordering transition temperature T_c, is characterized by a point where the maximum positive slope of susceptibility occurs (in χ vs T). In this experiment, however, the zero-field ac susceptibility was not carried out at an initial state ($M=0$, $H=0$) for $T<T_c$ because of the small remnant magnetization due to the domain structure. Furthermore, an amount of uncertain field, ± 1 Oe owing to the inaccuracy of the field measurement, could change the size and formation of domains. This effect will also blunt the sharpness of the peak.

The polycrystalline powder ac susceptibility as shown in Fig. 5 reflects a resultant susceptibility of the spin principle axes $\chi_{\text{powder}}=\frac{1}{3}(\chi_x+\chi_y+\chi_z)$. The order temperature T_c therefore, is not determined by the point at which a maximum of the susceptibility occurs. Fisher[44] showed that the temperature variation of the specific heat $c(T)$ of a uniaxial antiferromagnet is essentially the same as that of the temperature derivative of the product of the parallel susceptibility and temperature,

$$c(T)=A\frac{\partial(T\chi_\parallel)}{\partial T}=A\left[\chi_\parallel+T\frac{\partial\chi_\parallel}{\partial T}\right],$$

where A is a slowly varying function of temperature. This expression implies that any specific-heat anomaly related to a transition will be associated with a similar anomaly in $\partial(T\chi_\parallel)/\partial T$ or $\partial\chi_\parallel/\partial T$. Thus, the transition temperature T_c is associated with a positive infinite or maximum (usually observed in experiments) gradient in the parallel susceptibility. For most of the antiferromagnetic copper layer compounds, the perpendicular susceptibility observed remains approximately constant below $T_c(\partial\chi_\perp/\partial T\approx 0)$. The temperature derivative of the zero-field susceptibility of the powder $\partial(T\chi_p)/\partial T$ then is mainly taken as characteristic of $\partial(T\chi_\parallel)/\partial T$. Thus, the values of T_c can be estimated corresponding to the positive maximum slope of $\chi_p T$ vs T. Figures 6(a) and 6(b) show the results of numerically differential plots, $\Delta(\chi_p T)/\Delta T$ vs. T, for the $n=1$. Using this method the transition temperatures for $n=1$ and 2 have been found to be 12.81 ± 0.05 K and 12.85 ± 0.05 K, respectively. For the $n=3$ compound, there is no well-defined positive peak in $\partial\chi_p/\partial T$ vs T so the value of T_c was estimated to be 10.2 ± 0.2 K corresponding to the peak of χ_p vs T.

B. Single-crystal EPR linewidth analysis

Three contributions to the EPR linewidths have been recognized in $A_2[CuX_4]$ layer perovskite compounds. These include (1) spin anisotropies,[6] which are enhanced

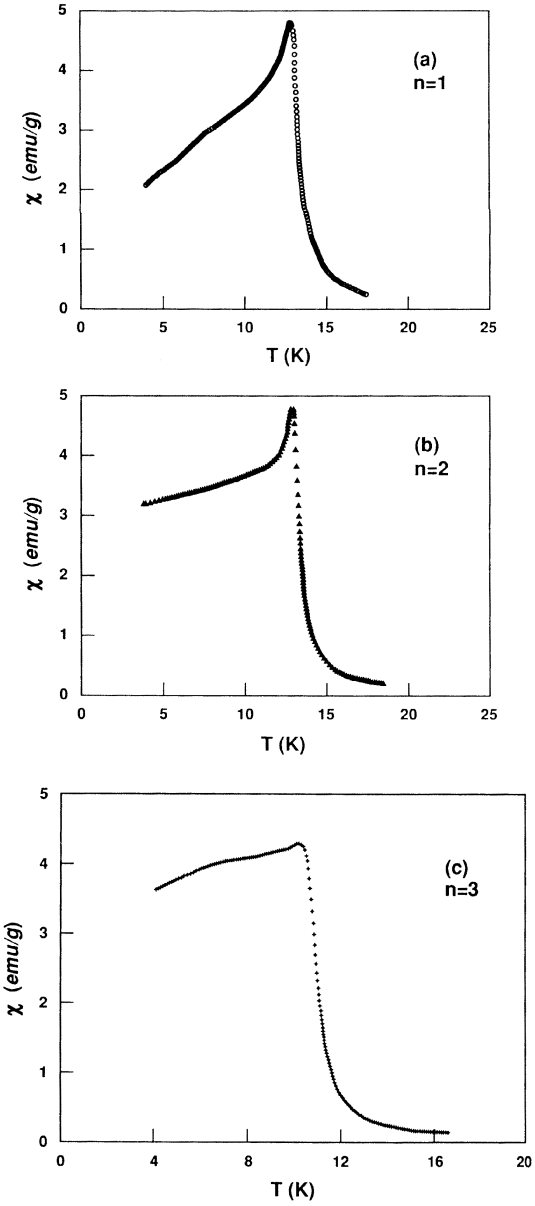

FIG. 5. Zero-field ac susceptibility vs temperature for the powdered samples.

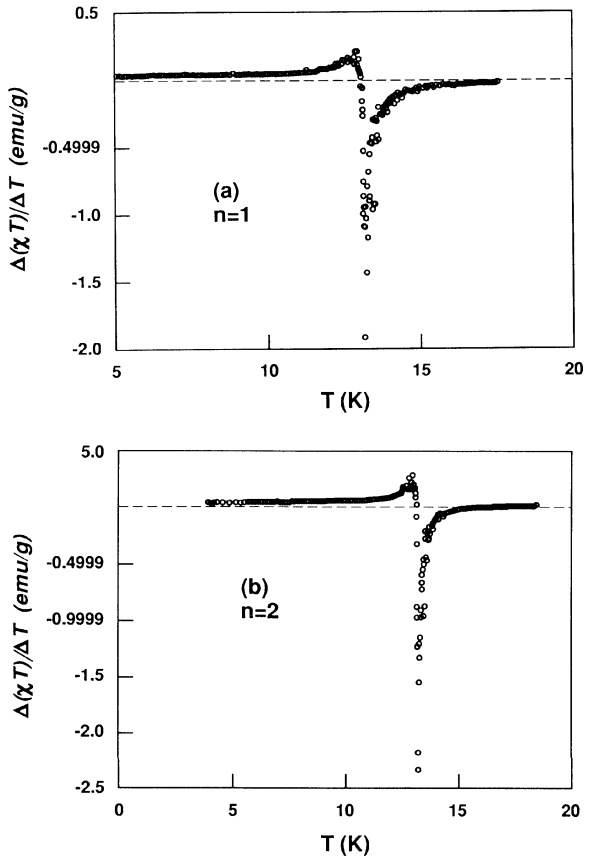

FIG. 6. Numerically differentiated plots $\Delta(\chi T)/\Delta T$ vs T taken from the zero-field ac susceptibility data (Fig. 5). $T_c = 12.81 \pm 0.05$ and $T_c = 12.85 \pm 0.05$ K are estimated corresponding to the peaks in (a) and (b) for $n = 1$ and $n = 2$ samples, respectively.

by phonon modulation effects,[45] (2) two-dimensional spin diffusion effects,[45] and (3) overlapping resonance lines due to magnetically inequivalent layers.[46] The spin anisotropies produce an angular dependent broadening, proportional to the second power of their magnitudes, which has a strong linear temperature dependence. The spin-diffusion effects, produced by long-time relaxation process, lead to a $(3\cos^2\theta - 1)^2$ angular dependence. The theoretical background of these effects has recently been reviewed, and applied to the corresponding $[C_6H_5(CH_2)_nNH_3]_2CuCl_4$ series.[41]

The conditions under which these three effects are seen can be summarized as follows: Inequivalent site broadening will be observed only when J' is extremely small compared to the g anisotropy, magnetically inequivalent layers are present, and linewidths are less than or equal to the g shifts between inequivalent sites. The spin-diffusive behavior will be observed only when J' is small and spin anisotropies are small. Since the magnitude of the spin anisotropies is proportional to J, among other things, they will dominate the linewidth when the intralayer coupling is large. In general, the anisotropies (and J values) are large enough for the bromide layer perovskites that spin-diffusive effects are not seen. Inequivalent site broadening is also more difficult to observe in the bromide series since (1) the inherent linewidths are generally larger than in the corresponding chloride salts, and (2) the g anisotropy is substantially smaller so the effect is smaller. From the crystal symmetry, it is possible that site broadening can occur in all three compounds, but evidence for it is observed only for the $n = 3$ salt.

Soos *et al.*[6] have shown that the spin anisotropy contribution to the EPR linewidths can be written as

$$\Delta H = \frac{2}{\sqrt{3}\omega_{\text{eff}}}[M_2^A(\theta,\phi)F_A(\beta J_0) + M_2^S(\theta,\phi)F_S(\beta J_0)]\frac{\chi_c}{\chi(T)} , \tag{1}$$

with $\beta = 1/kT$, $F_A(\beta J_0)$ and $F_S(\beta J_0)$ are correlation functions for the antisymmetric and symmetric exchange anisotropies, χ_c is the Curie susceptibility, and $\chi(T)$ the observed susceptibility. For the CuX_4^{2-} layer of the type shown in Fig. 1, they obtain the following second moments:

$$M_2^A(\theta,\phi) = \frac{zd_x^2(1+\sin^2\theta\cos^2\phi)}{16} + \frac{zd_y^2(1+\sin^2\theta\sin^2\phi)}{16} + \frac{zd_z^2(1+\cos\theta)}{16} \tag{2}$$

and

$$M_2^S(\theta) = \frac{zD^2(1+\cos^2\theta)}{8} , \tag{3}$$

where d_x, d_y, d_z are the components of the antisymmetric exchange vector **d**, D is the symmetric exchange, and z is the number of nearest neighbors. The experimentally measured linewidth at a temperature T is given by

$$\Delta H(\theta,\phi,T) = \frac{2}{\sqrt{3}\omega_{\text{eff}}}\left[\left[\frac{zd_x^2(1+\sin^2\theta\cos^2\phi)}{16} + \frac{zd_y^2(1+\sin^2\theta\sin^2\phi)}{16} + \frac{zd_z^2(1+\cos^2\theta)}{16}\right]\left[F_A\frac{\chi_c}{\chi(T)}\right] + \frac{zD^2(1+\cos^2\theta)}{8}F_s\frac{\chi_c}{\chi(T)}\right] . \tag{4}$$

Since the d_z^2 and D^2 terms have the same angular dependence, they cannot be determined independently (at least from measurements at a single temperature). The experimental data are thus fitted to an equation of the form

$$\Delta H(\theta,\phi,T)=A+B_1\cos^2(\theta-\theta_0)+B_2\sin^2(\theta-\theta_0)\cos^2(\phi-\phi_0)\ , \quad (5)$$

where θ_0 and ϕ_0 specify the orientation of the anisotropy with respect to the crystal coordinate system.

It is conventional to set $\omega_{\text{eff}}\sim J_0/\hbar$. This is only valid at low temperatures where other contributions—e.g., phonon modulation effects—to the temperature dependence of the linewidths can be neglected. This is generally not valid for the bromide series. In this case it is possible only to calculate the ratios, e.g., d_x^2/d_y^2 or $(d_z^2+RD^2)/d_y^2$, where $R=2F_s/F_A$. The results of the magnetic anisotropy analyses are given in Table II.

The crystal g factors are nearly axial and qualitatively the g values vary roughly from 2.04–2.05 normal to the layer (g_c in Table III) to 2.08–2.09 in the plane of the layer (g_a, g_b in Table III) as can be seen in Fig. 7 for the data in the ac plane of the $n=1$ salt. Because of the antiferrodistortive arrangement of the planar $CuBr_4^{2-}$ anions (Fig. 1), the following relations hold approximately (neglecting tilting of the $CuBr_4^{2-}$ anions):

$$g_c^*(\text{crystal})\sim g_\perp(\text{single ion})$$

and

$$g_a(\text{crystal})\sim g_b(\text{crystal})\sim \tfrac{1}{2}g_\perp(\text{single ion})+\tfrac{1}{2}g_\parallel(\text{single ion})\ .$$

Thus we have, approximately, $g_\perp$ (single ion)$\sim$2.04 and $g_\parallel$ (single ion)$\sim$2.14. Quantitatively, the g values are fitted quite well by the relation

$$g(\theta,\phi)=g_0+g_1\cos^2(\theta-\theta_0')+g_2\sin^2(\theta-\theta_0')\cos^2(\phi-\phi_0')\ . \quad (6)$$

The values of θ_0' and ϕ_0', which correct for any crystal misalignment, were small ($<5°$). The small, but significant, difference in g_a and g_b for the $n=2$ salt is due to the unequal a and b lattice constants.

The linewidth behavior is somewhat different for all three compounds. The one common feature is a very strong temperature dependence, attributable to a strong phonon modulation of the spin anisotropies due to the large spin-orbit coupling of the bromide ion.[45]

For the $n=1$ compounds, the room-temperature linewidths are broad in all planes ($\Delta H\approx 600-800$ G) and are axially symmetric about the c axis, with $\Delta H_c=790\pm25$ G and $\Delta H_a=\Delta H_b=675\pm25$ G. At liquid-nitrogen temperature, the linewidths are considerably narrowed ($\Delta H\sim 75$ G), and remain isotropic in the plane of the layer, with $\Delta H_a=\Delta H_b=72.0\pm2.5$ G and $\Delta H_c=80.5\pm2.5$ G. The data for the ac plane are shown in Fig. 8. Since there is no ϕ dependence, it is required that $|d_x|=|d_y|$. The fact that $\Delta H_c>\Delta H_a$, ΔH_b implies that the $|D|$ and $|d_z|$ contributions dominate over the $|d_x|$ and $|d_y|$ contributions to the linewidths. This is normal behavior for the copper(II) bromide layer perovskites.

For $n=2$, the room-temperature linewidths are also broad ($\Delta H\sim 667-775$ G). In the plane of the layer (the ab plane) there is some structure in the spectrum. The structure does not change with orientation. The overall linewidth in the ab plane is broader ($\Delta H\sim 800$ G) when compared to the linewidths in the ac and bc planes ($\Delta H\sim 665-775$ G). At the liquid-nitrogen temperature, the linewidths are considerably narrowed ($\Delta H\sim 70-90$ G). There are no observable contributions to linewidth either from spin diffusion or from the magnetically inequivalent sites in the unit cell. In the ab plane (the plane of the layer), there is a strong ϕ dependence, in addition to the θ dependence.

A composite plot of the angular variation of the linewidth in all planes for the $n=2$ salt is shown in Fig. 9 where the solid line depicts the best fit of the data with $A=70.9$ G, $B_1=16.9$ G, and $B_2=12.4$ G, and the corresponding plot for the g factor is shown in Fig. 10. As is clear from Figs. 9 and 10, the general trend of the angular variation of the linewidth and the g factor is the same as for the $n=1$ compound, i.e., as the linewidth increases, the g factor decreases and vice versa. Because of the ϕ dependence, $|d_x|$ and $|d_y|$ are no longer equal, and detailed analysis yields

$$|d_x/d_y|=1.31\ .$$

The dominance of the $|d_z|$ and $|D|$ components is also confirmed (Table II).

The EPR data for the $n=3$ compound are quite unusual. At room temperature the lines show some structure at most of the orientations in each plane. In the ac and bc planes, the structure in the line shifts with the orientation. In the plane of the layer (ab plane), the structure does not shift, but is more pronounced than in the ac and bc planes. The structure seems to be due to the overlap-

TABLE III. Summary of EPR results on 2-D layer perovskite systems at 77 K.

		Parameters from $\Delta H(\theta,\phi)$ fit Gauss			g values along crystallographic axes			ΔH values along crystallographic axes (G)		
Compound	J/k_B (K)	A	B_1	B_2	g_a	g_b	g_c	ΔH_a	ΔH_b	ΔH_c
$n=1$	25.0	72.0	9.0	0.0	2.090	2.090	2.042	72	72	81
$n=2$	22.7	73.2	14.3	9.4	2.087	2.096	2.055	83	74	88
$n=3$	21.1				2.087	2.086	2.050	160	275	185

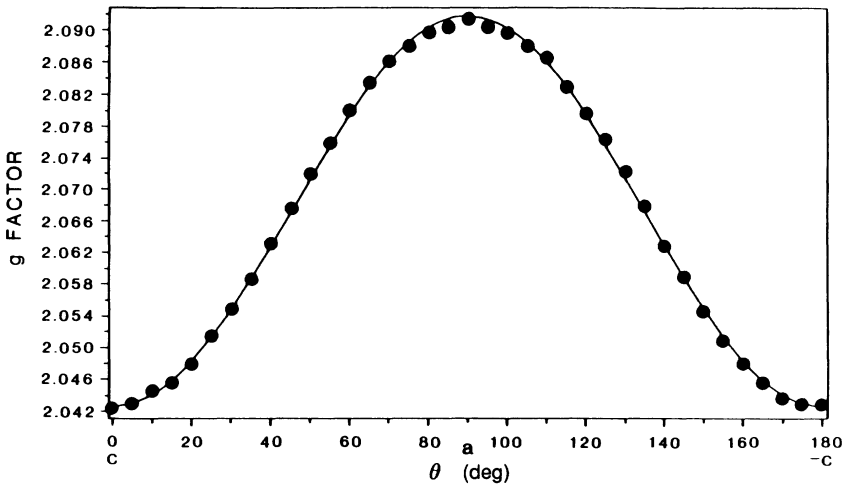

FIG. 7. Angular variation of the g factor in the ac plane of the $n=1$ salt at 77 K. Solid line is the best fit to Eq.(6).

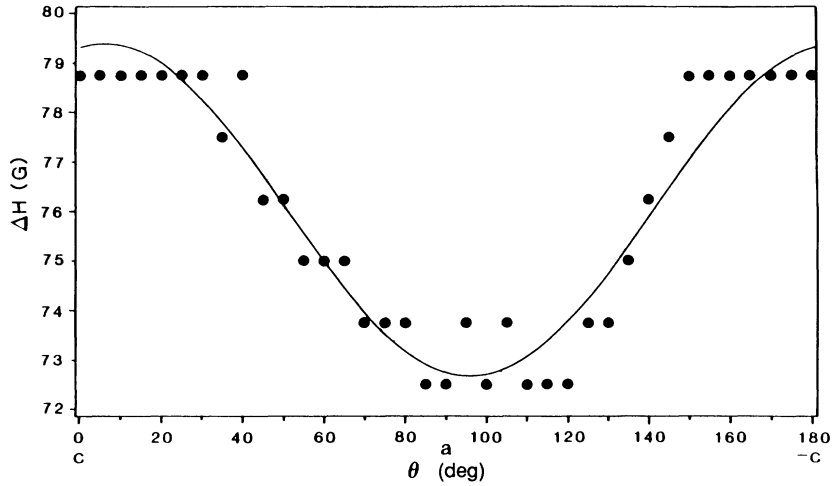

FIG. 8. Angular variation of ΔH in the ac plane of the $n=1$ salt at 77 K. Solid line is the best fit to Eq.(5).

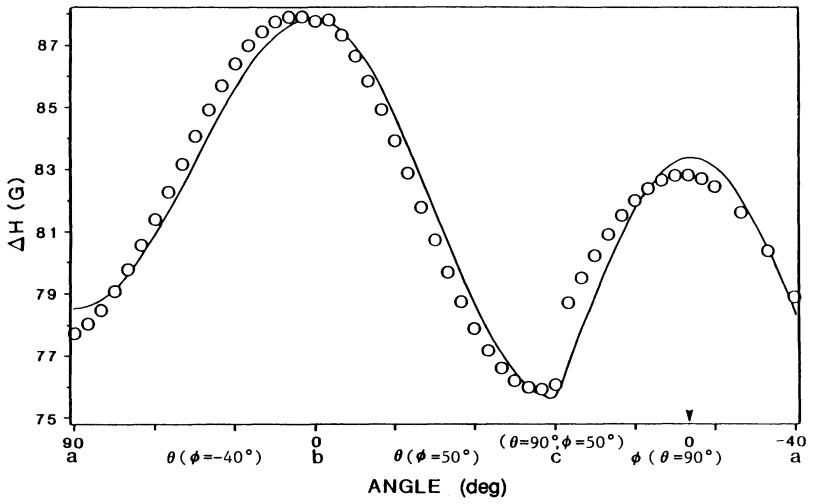

FIG. 9. Composite plot of the angular variation of ΔH for the $n=2$ salt at 77 K. The solid line is the best fit to Eq.(5).

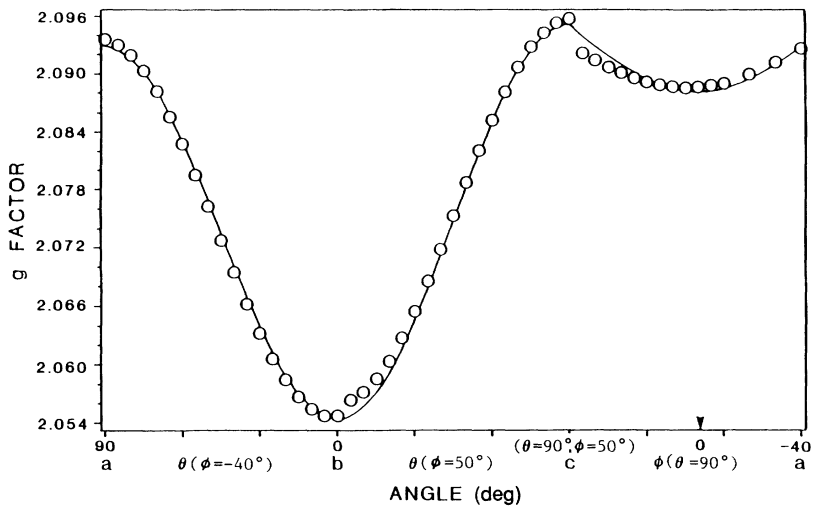

FIG. 10. Composite plot of the angular variation of the g factor for the $n=2$ salt at 77 K. The solid line is the best fit to Eq.(6).

ping lines from magnetically inequivalent sites. The linewidths are somewhat broader than those of the other bromide compounds ($\Delta H \sim 900$ G).

At the liquid-nitrogen temperature, the linewidths are now much broader than the linewidths of the other two salts ($\Delta H \sim 250$ G as compared to $\Delta H \sim 85$G). In the bc plane the linewidth anisotropy and the g-factor anisotropy follow each other while in the ac plane the ΔH anisotropy and the g factor anisotropy proceed in opposition to each other (as is the case for the other two salts in this series). In the plane of the layer (the ab plane) there is a strong ϕ dependence of both the linewidth and the g factor. The linewidth and g factor anisotropies proceed in opposition to each other.

In the case of the $n=1$ and $n=2$ salts, the isotropic exchange J is 25.0 and 22.7 K, respectively, and the linewidths at liquid N_2 are temperature$\sim$85 G. In the case of the $n=3$ compound, $J=21.13$ K and the linewidths are $\sim$225 G. Based on the J values, we should expect similar contributions to linewidths from antisymmetric and symmetric exchange for all these compounds. Since the linewidths are too broad to be explained in terms of $|d|$ and D alone, it must be accumed that we have contributions to the linewidths from magnetically inequivalent sites in all planes. This is expected from the crystal structure information, and is consistent with the behavior of the corresponding chloride salt, where it was possible to resolve absorption due to inequivalent sites in certain orientations.[41]

C. Magnetic critical behavior and exponents of powdered samples

The strong ferromagnetic intralayer interactions which have been found in these compounds yield ferromagnetic behavior for the powdered samples. Since the magnetic properties of polycrystalline powder reflect a resultant (average) effect along the crystal axes, the antiferromagnetic interlayer coupling, even if it is very small, as well as the spin canting due to the antisymmetric exchange will cause the ferromagnetic behavior of these powdered samples to deviate from that of usual 2D and 3D ferromagnets. This difference should be significant around a critical point.

For the simple ferromagnet, the critical exponents β, δ, and γ, and γ' which characterize the ferromagnetic-paramagnetic transition along the critical isochore, critical isotherm, and coexistence lines of approach to the critical point are defined in terms of the reduced temperature $\varepsilon=(T-T_c)/T_c$ as follows: spontaneous magnetization, $M_s \propto (-\epsilon)^{\beta}$, $T \rightarrow T_c (T<T_c)$ at $H=0$; critical isothermal magnetization, $M \propto H^{1/\delta}$, $H \rightarrow 0$, at $T=T_c$; initial susceptibility, $\chi_0 \propto (-\epsilon)^{-\gamma'}$, $T \rightarrow T_c$ $(T<T_c)$ at $H=0$, and $\chi_0 \propto (\epsilon)^{-\gamma}$, $T \rightarrow T_c$ $(T>T_c)$ at $H=0$.

There are several ways to determine the values of β, γ, δ, and T_c experimentally. The most direct method is to analyze the data of spontaneous magnetization, initial susceptibility, and critical isotherm. To do this, we have plotted the data in terms of ln M_s vs ln$|1-T/T_c|$, ln χ_0 vs ln $|1-T/T_c|$, and ln M_c vs ln H to obtain straight lines near the critical point. The advantage of this method is that there is only one nonlinear adjustable parameter, T_c.

To estimate the critical exponent γ, the initial ac susceptibility (Fig. 5) data were replotted in terms of ln χ_0 vs ln (T/T_c-1) for $T>T_c$ as shown in Figs. 11(a) and 11(b) for the $n=1$ and 2 compounds, respectively. Thus, $\gamma=1.39$ was estimated from the slope of the visually best-fit straight line near T_c for $n=1$ and 2 compounds. The value of γ estimated here for these compounds is close to that given by the 3D Heisenberg $S=\frac{1}{2}$ model[47] and slightly smaller than that given by the 2D XY model.[48]

The value of critical exponent δ can be given by the inverse slope of ln (M_c) vs ln(H). However, a systematic error could be present in the determination of δ owing to the inaccuracy of measurement of T_c since the measurement of critical isothermal magnetization M_c should be carried out exactly at $T=T_c$. To avoid this difficulty, the measurements of sets of isotherms near T_c were made. Figures 12(a), 12(b) and 12(c) show the results of the mea-

surements on the $n=1$, 2, and 3 compounds, in terms of a ln M_c vs ln H plot, in the field range $H<1400$ Oe. At relativity high fields (700 Oe $<H<4000$ Oe), the isothermal data near T_c are shown in Figs. 13(a), 13(b), and 13(c) for $n=1$, 2, and 3, respectively. According to the definition of the critical exponent δ, the critical isotherm is the one which is fitted as closely as possible by a straight line whose inverse slope gives the value of δ. It is clear in Figs. 12 and 13 that there is no linearity to be found among the sets of isotherms. The data indicate that the magnetization at low-field range is suppressed when compared to usual ferromagnets so that the conventional power law does not hold in the critical region. This feature will be clearly seen when the scaling law is applied to analyze the data.

The scaling hypothesis[49] gives rise to functional relations among the critical exponents and makes specific predictions concerning the general form of the equations of state[50–56] which have been used with success in a large number of critical phenomena investigations on various ferromagnetic materials.[51,53,54,56–65]. One of the most useful and important equations of state which scaling properties must satisfy is given as

$$(H/M)^{1/\gamma}=at+bM^{1/\beta}\ , \tag{7}$$

the so-called modified Arrott plot or Arrott-Noakes plot.[51] Here a and b are constants and t is reduced temperature T/T_c-1. By properly choosing the values of γ

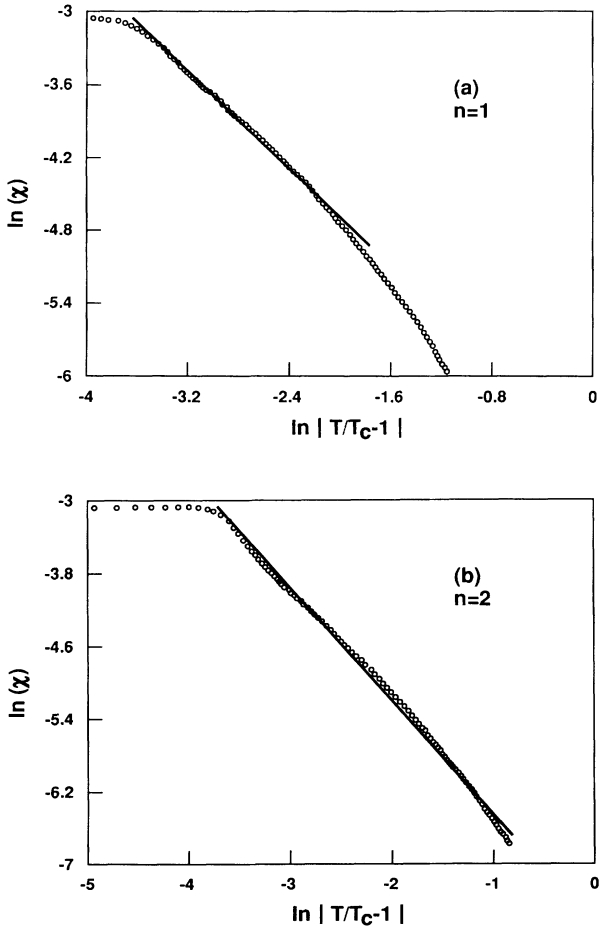

FIG. 11. ac initial susceptibility plotted in terms of ln(M/H) vs ln(T/T_c-1). Solid lines are fitted for $n=1$ and 2 compounds with $\gamma=1.39$.

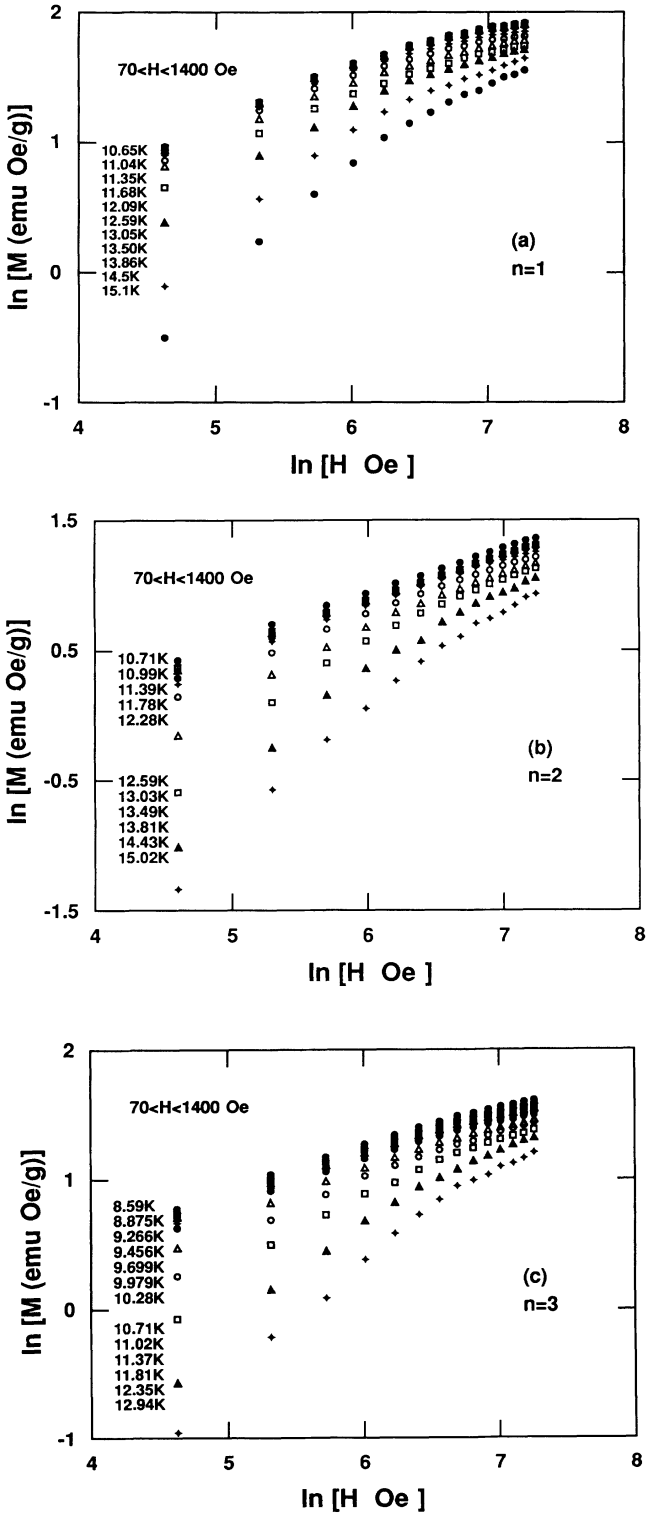

FIG. 12. Isothermal magnetization in fields $70<H<1400$ Oe plotted in terms of ln(M) vs ln(H).

and β, plots of $(H/M)^{1/\gamma}$ vs $M^{1/\beta}$ fall on a set of parallel straight-line isotherms in which a line passing through the origin corresponds to $T_c(t=0)$. This property can be used to determine the values of β, γ, and T_c. In this manner, the extrapolation difficulties usually related to the asymptotic analysis from measurements of spontaneous magnetization, initial susceptibility, and critical isotherm are avoided. The equation of state, Eq.(7), has been applied with success in a large number of critical phenomena investigations on various ferromagnetic materials. For the most simple isotropic 3D ferromagnets, the isotherms in such a plot yield linearity well up into even the high-field region.

We have also applied this static equation of state to carefully analyze the isotherm data of our layer compounds. By choosing $\gamma=1.39$ and varying β systematically, with the value of δ given by the scaling relation $\gamma=\beta(\delta-1)$, it is found that the isotherms near the T_c never fall on a set of parallel straight lines in the Arrott-Noakes plot in a low-field region. In principle, it is possi-

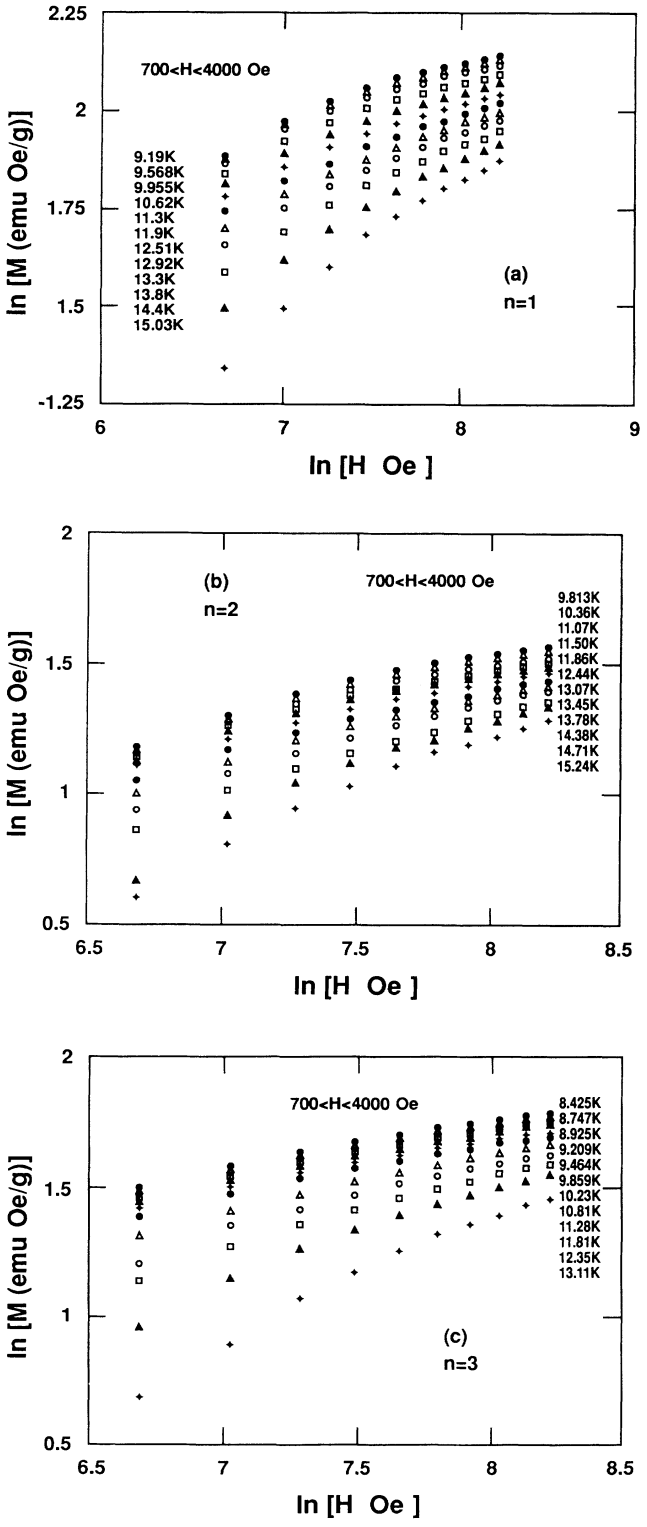

FIG. 13. Isothermal magnetization in fields $700<H<4000$ Oe plotted in terms of $\ln(M)$ vs $\ln(H)$.

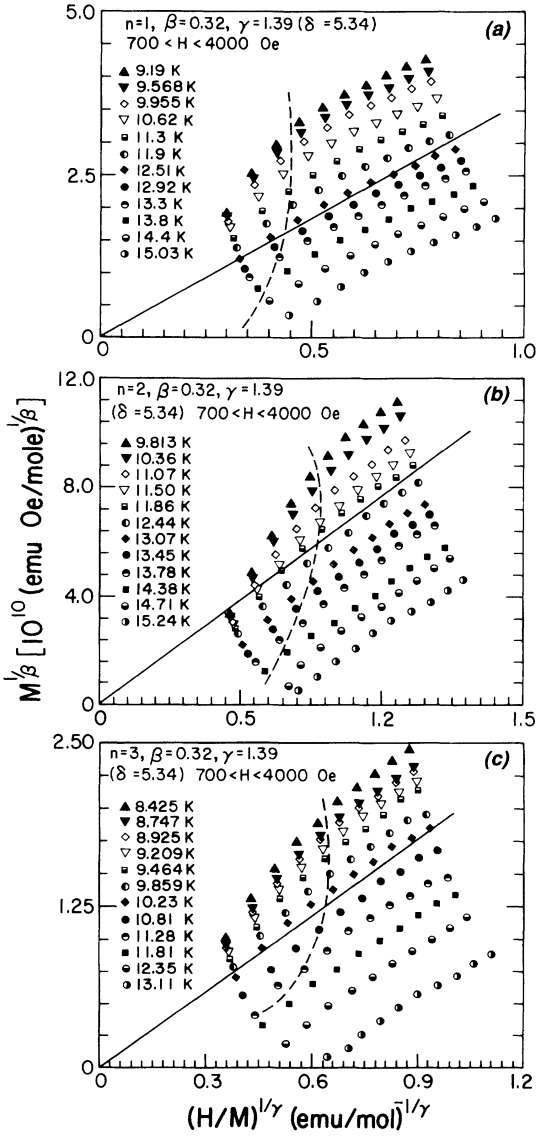

FIG. 14. The Arrott-Noakes plots with $\gamma=1.39$ and $\beta=0.32$ in fields $700<H<4000$ Oe. The dashed lines indicate that the magnetization starts to be suppressed as the field decreases so that the scaling law no longer holds.

ble to obtain parallel isotherm lines by varying both values of β and γ. However, the true values of β and γ should simultaneously satisfy three conditions: (1) best parallel isotherm lines in the Arrott-Noakes plot, (2) a line passing through the origin corresponding to the critical isotherm ($T=T_c$), and (3) Widom's scaling relation $\gamma=\beta(\delta-1)$. It is found that these conditions are not self-consistently satisfied here for these powder compounds. Figure 14 shows one of the results in Arrott-Noakes plot in the field range $700<H<4000$ Oe for these samples. It is clear in Fig. 14 that the isotherms are linear at relatively high fields, but at a certain low-field and low-temperature region, indicated as dashed lines in Fig. 14, the data no longer fall on a set of parallel straight lines in the Arrott-Noakes plot, which implies that magnetizations at low field are suppressed so that the static scaling hypothesis no longer holds. This behavior may mainly be caused by the existence of weakly antiferromagnetic interlayer ordering or by canting from the antisymmetric exchange. Nevertheless, this is the first example of the scaling analysis for the 2D layer systems. It is shown that since scaling invariance is not valid around the critical point, these powdered compounds cannot be classified as usual ferromagnets whose critical behavior is described by most of the 2D critical theories.

IV. CONCLUSION

The magnetic properties and critical behavior of the 2D layered ferromagnets $[C_6H_5(CH_2)_nNH_3]_2CuBr_4$ with $n=1$, 2, and 3 were studied. Magnetizations, susceptibilities, and EPR have been measured and strong ferromagnetic intralayer exchange couplings were found. The strong temperature dependence of the EPR linewidths is indicative of phonon modulation of the spin anisotropies as the principal broadening mechanism. Analysis of the angular dependence of the linewidth showed that the d_z component of the antisymmetric exchange, and the axial component D of the symmetric component, make the dominant contribution to the linewidths. The linewidths of these bromide salts are much larger than those in the corresponding chloride. The increased magnetic anisotropy present in the bromide salts is due to the larger spin-orbit coupling of bromide as compared to chlorine. The absence of a low-dimensional spin-diffusion contribution to the EPR linewidths in these bromide salts is due to dominance of the short-time contribution of the spin anisotropies to the correlation function. The critical exponents β, γ, δ, and transition temperatures T_c were estimated from the measurements of ac initial susceptibility and isothermal magnetization. A scaling law was applied to analyze the data of isothermal magnetization near T_c and it was found that in a certain low-field and low-temperature region the powder magnetizations are suppressed so that the scaling law no longer holds. This example of scaling analysis for these ferromagnetic 2D layer systems shows that their powders cannot be classified as usual simple ferromagnets whose critical behavior is described by most 2D critical-point theories.

ACKNOWLEDGMENTS

We would like to thank K. Ravindran for assistance with ac susceptibility measurements and Professor G. F. Tuthill, Professor H. V. Schmidt, and Professor G. V. Rubenacker for useful discussions and remarks. This work was supported by National Science Foundation Grant Nos. DMR-90-11072 and DMR-88-03382.

*Present address: Baker Laboratory of Cornell University, Ithaca, NY 14853.

[1]L. J. de Jongh and A. R. Miedema, Adv. Phys. **23**, 1 (1974).
[2]P. Bloembergen, Physica B **79**, 467 (1975); **81**, 205 (1976).
[3]G. P. Bloembergen and A. R. Miedema, Physica **75**, 205 (1974).
[4]H. von Känel, Physica B **96**, 167 (1979).
[5]L. J. de Jongh, Physica B **82**, 247 (1976).
[6]Z. G. Soos, K. T. McGregor, T. T. P. Cheung, and A. J. Silverstein, Phys. Rev. B **16**, 3036 (1977).
[7]D. B. Losee and W. E. Hatfield, Phys. Rev. B **10**, 212 (1974); **10**, 1122 (1974); Phys. Rev. Lett. **35**, 1665 (1975).
[8]H. van Kempen, F. H. Mischgofsky, and P. Wider, Phys. Rev. B **15**, 4386 (1977).
[9]L. O. Snively, G. F. Tuthill, and J. E. Drumheller, Phys. Rev. B **24**, 5349 (1981).
[10]L. O. Snively, D. N. Haines, K. Emerson, and J. E. Drumheller, Phys. Rev. B **26**, 5245 (1982).
[11]H. E. Stanley and T. A. Kaplan, Phys. Rev. Lett. **17**, 913 (1966).
[12]N. D. Mermin and H. Wagner, Phys. Rev. Lett. **17**, 1133 (1966).
[13]G. S. Rushbrooke and P. J. Wood, Mol. Phys. **1**, 257 (1958).
[14]V. L. Berezinskii, Zh. Eksp. Teor. Fiz. **59**, 907 (1970) [Sov. Phys. JETP **32**, 493 (1971)].
[15]L. J. de Jongh, P. Bloemergen, and J. H. P. Colpa, Physica **58**, 305 (1972).
[16]V. L. Berezinskii and A. Ya. Blank, Zh. Eksp. Teor. Fiz. **64**, 725 (1973) [Sov. Phys. JETP **37**, 369 (1973)].
[17]V. L. Pokrovskii and G. V. Uimin, Zh. Eksp. Teor. Fiz. **65**, 1691 (1973) [Sov. Phys. JETP **38**, 847 (1974)]; Phys. Lett. **45A**, 467 (1973).
[18]B. C. Gerstein, K. Chang, and R. D. Willett, J. Chem. Phys. **60**, 3453 (1974).
[19]L. J. de Jongh, Physica B **82**, 247 (1976).
[20]R. Navarro and L. J. de Jongh, Physica B **84**, 229 (1976).
[21]M. den Nijs, Phys. Rev. B **27**, 1674 (1983).
[22]D. A. Huse, Phys. Rev. B **30**, 3908 (1984).
[23]E. Seiler and I. O. Stametesca, Nucl. Phys. **B305**, 623 (1988).
[24]M. Barma and M. E. Fisher, Phys. Rev. Lett. **53**, 1935 (1984).
[25]I. Affleck, Phys. Rev. Lett. **55**, 1355 (1985).
[26]B. Nienhuis and H. J. F. Knops, Phys. Rev. B **32**, 1872 (1985).
[27]S. Chakravarty, B. I. Halperin, and D. R. Nelson, Phys. Rev. Lett. **60**, 1057 (1988).
[28]H. Kunz and F. Y. Wu, J. Phys. A **21**, L1141 (1988).
[29]C. M. Naon, J. Phys. A **22**, L207 (1989).
[30]M. T. Batchelor and H. W. J. Blöte, Phys. Rev. B **39**, 2391 (1989).
[31]S. Chakravarty, B. I. Halperin, and D. R. Nelson, Phys. Rev. B **39**, 2344 (1989).
[32]D. S. Fisher, Phys. Rev. B **39**, 11 783 (1989).

[33]V. S. Potsenko and V. A. Fateev, Nucl. Phys. **B240**, 312 (1984).
[34]A. A. Belavin, A. M. Polyakov, and A. B. Zamolodchikov, Nucl. Phys. **B241**, 333 (1984).
[35]D. Friedan, Z. Qiu, and S. Shenker, Phys. Rev. Lett. **52**, 1575 (1984).
[36]J. L. Cardy, in *Phase Transitions and Critical Phenomena,* edited by C. Domb and J. L. Lebowitz (Academic, New York, 1987), Vol. 11, p. 55.
[37]P. P. Martin, J. Phys. A **22**, 3991 (1989).
[38]H. W. J. Blöte and B. Nienhuis, J. Phys. A **22**, 1415 (1989).
[39]A. Dupas, K. Le Dang, J. P. Renard, P. Veillet, A. Daoud, and R. Perret, J. Chem. Phys. **65**, 4099 (1976).
[40]W. E. Estes, D. B. Losee, and W. E. Hatfield, J. Chem. Phys. **72**, 630 (1980).
[41]B. R. Patyal and R. D. Willett, Magn. Reson. Rev. (to be published).
[42]R. D. Willett, Acta Crystallogr. C **44**, 565 (1990).
[43]J. P. Steadman and R. D. Willett, Inorg, Chim. Acta **4**, 367 (1970).
[44]M. E. Fisher, Proc. R. Soc. London, Ser. A **254**, 66 (1960); Philos. Mag. **7**, 1731 (1962).
[45]R. D. Willett and R. J. Wong, J. Magn. Reson. **42**, 446 (1981); R. D. Willett, F. H. Jardine, I. Rouse, R. J. Wong, C. P. Landee, and M. Numata, Phys. Rev. B **24**, 5372 (1981).
[46]R. J. Wong, R. D. Willett, and J. E. Drumheller, J. Chem. Phys. **74**, 6018 (1981).
[47]G. S. Rushbrooke, G. A. Baker, and P. J. Wood, in *Phase Transitions and Critical Phenomena,* edited by C. Domb and M. S. Green (Academic, New York, 1974) Vol. 3, p. 322.
[48]D. D. Betts, in *Phase Transitions and Critical Phenomena,* edited by C. Domb and M. S. Green (Academic, New York, 1974) Vol. 3, p. 570.
[49]A. Hankey and H. E. Stanley, Phys. Rev. B **6**, 3515 (1972).
[50]B. Widom, J. Chem. Phys. **43**, 3898 (1965).
[51]A. Arrott and J. E. Noakes, Phys. Rev. Lett. **19**, 786 (1967).
[52]B. D. Josephson, J. Phys. C **2**, 1113 (1969).
[53]J. T. Ho and J. D. Litster, Phys. Rev. Lett. **22**, 603 (1969).
[54]S. Milosevic and H. E. Stanley, Phys. Rev. B **5**, 2526 (1972).
[55]J. Rudnick and D. R. Nelson, Phys. Rev. B **13**, 2208 (1976).
[56]M. Barmatz, P. C. Hohenberg, and A. Kornblit, Phys. Rev. B **12**, 1947 (1975).
[57]J. S. Kouvel and M. E. Fisher, Phys. Rev. **136**, A1626 (1964).
[58]P. Schofield, J. D. Litster, and J. T. Ho, Phys. Rev. Lett. **23**, 1098 (1969).
[59]R. Krasnow and H. E. Stanley, Phys. Rev. B **8**, 332 (1973).
[60]M. Vicentini-Missoni and J. M. H. L. Sengers, Phys. Rev. Lett. **22**, 389 (1969).
[61]R. Jesser, A. Bieber, and R. Kuentzler, J. Phys. (Paris), **42**, 1157 (1981); **44**, 631 (1983).
[62]Y. Yeshurun, M. B. Salamon, K. V. Rao, and H. S. Chen, Phys. Rev. B **24**, 1536 (1981).
[63]K. Westerholt, H. Bach, and R. Romer, J. Magn. Magn. Mater. **45**, 252 (1984).
[64]U. Kobler, K. Fischer, W. Zinn, and H. Pink, J. Magn. Magn. Mater. **45**, 157 (1984).
[65]S. N. Kaul, J. Magn. Magn. Mater. **53**, 5 (1985).